Journal of Applied Polymer Science

WILEY

Applied Polymer SCIENCE

RESEARCH ARTICLE OPEN ACCESS

3D-Printable Polymer Filters for the Selective Complexation of Silver Ions

Timo Koswig[1,2] | Josefine Meurer[1,2] | Thomas Bätz[1,2] | Oswald Müschke[1,2] | Stefan Zechel[1,2] | Martin D. Hager[1,2,3] | Ulrich S. Schubert[1,2,3]

[1]Laboratory of Organic and Macromolecular Chemistry (IOMC), Friedrich Schiller University Jena, Jena, Germany | [2]Jena Center for Soft Matter (JCSM), Friedrich Schiller University Jena, Jena, Germany | [3]Helmholtz Institute for Polymers in Energy Applications Jena (HIPOLE Jena), Jena, Germany

Correspondence: Ulrich S. Schubert (ulrich.schubert@uni-jena.de)

Received: 15 August 2024 | **Revised:** 8 November 2024 | **Accepted:** 12 November 2024

Funding: This work was supported by Carl Zeiss Stiftung (Durchbrüche 2019).

ABSTRACT

This study presents the fabrication of polymeric filters, which are able to selectively bind silver ions from aqueous solution. Those filters are fabricated within an easy approach via 3D-digital light processing (DLP)-printing enabling a tailor-made design. In first order, an acrylamide containing a benzo-trithiacrown-ether (BTCE) functionality is synthesized. This monomer is further 3D-printed via layer by layer photo-polymerization together with commercially available comonomers, resulting in polymer networks containing the BTCE-groups in their side chains as selective binding moiety for silver ions. Within isothermal-titration calorimetry (ITC) measurements, the complexation abilities of the BTCE to bind the Ag^+ ions are determined. Furthermore, the resulting 3D-printed filters are investigated regarding their complexation behavior, in a detailed fashion applying inductively coupled plasma optical emission spectroscopy (ICP-OES).

1 | Introduction

Nowadays, the topics "waste-reduction" and "recycling" are playing more and more important roles in society [1–3]. Both points are highly important to become more environmentally friendly and, therefore, save the planet for future generations [4, 5]. Additionally, humanity is slowly approaching a point at which resources are increasingly exhausted [6, 7]. In particular, this concerns the field of metals and heavy metals, which are required in many areas and technologies [8]. To overcome this, recycling and recovery of those materials is not just beneficial and environmentally friendly, moreover it is necessary to cover the requirements of the future [8]. However, commonly used metal recycling techniques today are mostly based on thermal melting processes, resulting in a low selectivity and high energy consumption, which makes it economically and environmentally questionable [8]. Consequently, more selective methods with a lower energy consumption need to be investigated to separate precious metals.

In 2017 Haukka et al. presented the fabrication of 3D-printed filters, which were able to selectively bind gold-ions from electronic waste [9]. Within this approach, it was possible to recover this valuable raw material, to separate it from other metal-ions and, therefore, to recycle it in a sufficient manner [9]. Similarly, Repo et al. 3D printed a porous filter which selectively binds and recovers copper [10]. Furthermore, also platinum and palladium have already been recovered from electronic waste selectively by Haukka et al. [11].

Among others, silver is applied in electronics, photography, and mirrors. However, as a precious metal it is expensive. Consequently, the goal of this study was to adapt the promising concept of 3D-printed filters for the selective recovery of

Timo Koswig and Josefine Meurer contributed equally to this article.

silver-ions. The idea was to 3D-print a filter, based on a polymer containing ligands in its side chains, which are able to selectively form complexes with Ag^+ ions.

The fabrication of those compounds via DLP-printing features several advantages. In general, 3D-printing is of increasing interest due to a time and cost saving production process [12, 13]. A prototype for a new product can easily be modeled utilizing computer aided design (CAD) software [14, 15] and printed within hours [16]. Function, stress, and fitting can be adjusted without the classical approach based on cutting based-machinery or injection molding [17]. Furthermore, for catalytic applications, shapes with a high surface area can easily be investigated, modified, and optimized [18]. Moreover, 3D printed filters are beneficial, as noble elements can be separated directly from the diluted leachate without tedious preprocessing [9].

The presented approach utilizes DLP-printing technology. This technique utilizes light from a projector to cure the raw resin in each layer all at once in a photo polymerization process [19]. Advantages of this process are its accuracy compared to fused deposition modeling (FDM), which is based on melting and extrusion of thermoplastics [20, 21], and its velocity compared to stereolithography (SLA), which uses a computer-controlled laser beam for photopolymerization to cure each layer step by step [14, 16]. Komissarenko et al. for instance used DLP printing for the fabrication of scandia-stabilized zirconia ceramic parts which can be used as electrolyte material in solid oxide fuel cells [22]. As polymers, typically acrylates or acrylamides are printed via DLP, which mostly contain a crosslinker, resulting in a stable polymer network. This stability is also important for the presented approach, in which the material should act as a filter. For different applications the resin can be modified with other substances, for example, to yield in acrylonitrile butadiene styrene (ABS)-like resins, with the strength and chemical inertness of ABS.

2 | Results and Discussion

As mentioned before, the ligand side chains in the printed polymers represent the key part for the desired complexation abilities. For this reason, a ligand able to selectively bind silver ions had to be chosen. Benzo-15-trithiacrown-5 (BTCE) is known to exhibit excellent abilities to selectively bind those ions featuring a soft Lewis acid character [23–25]. Based on the ring size and the soft Lewis base character of the sulfur, they represent a suitable counterpart to Ag^+-ions [26]. The BTCE-ligand could already be successfully utilized for cation recognition and sensing [24]. Already in 1985, Kimura and co-workers investigated the synthesis of BTCE containing polymers and their binding abilities [27].

The idea of this current study, is mainly based on the implementation of the BTCE-ligand into the polymeric material of DLP-printed filters. Applying this approach, it is possible to combine on the one hand the fabrication of polymers, which are able to recover silver ions from aqueous solutions, and on the other hand to design the shape of those filters in a simple way and a tailor-made manner via the DLP printing process.

2.1 | Synthesis of the Benzo-15-Trithiacrown-5-Ether Monomer

For the fabrication of the filters, it was firstly required to synthesize a benzo-15-trithiacrown-5-ligand monomer, which can be photopolymerized later. Consequently, an acrylamide functionality was chosen as monomeric unit, since these polymerize very fast and are often applied in DLP-processes [28–30]. The synthesis of this monomer is presented in Scheme 1 and was performed partially according to literature procedures, which have further been adapted and modified in some reaction steps [27].

The synthesis is mainly based on available and rather cheap chemicals and started with a Williamson-ether-synthesis of catechol and 2-chloroethanol, two commercially available and cheap chemicals, with sodium hydroxide as base. Applying gel chromatography, compound **1** could be obtained, which was characterized via nuclear magnetic resonance (NMR) spectroscopy (all NMR-spectra recorded can be found in Figure 1 as well as in the Supporting Information) as well as elemental analysis (EA). In the second reaction step, the two hydroxyl groups of **1** were transformed into chloride substituents via chlorination, utilizing thionyl chloride in pyridine to yield **2**, which was characterized applying NMR spectroscopy as well as EA. Within the next reaction step, a nitro-group was introduced at the aromatic ring (**3**) utilizing a combination of nitric and acetic acid. Subsequently, the 2-nitrobenzo-15-trithi acrown-5-ether (**4**) was gained by adding 2,2′-thiodiethanthiol under basic conditions.

Afterwards, the nitro-group was reduced (**5**) utilizing tin (II) chloride under hydrochloric acid conditions. During the reduction of the nitro-group, the formerly yellow colored solution turned colorless. Compound **5** was utilized without further characterization and purification, due to its reactivity and, therefore, rather low stability. Finally, the reaction with acryloyl chloride under the presence of triethylamine as base resulted in the desired monomer **6**. The successful synthesis of the monomer was proven by NMR spectroscopy, high resolution–electrospray ionization–mass spectrometry (HR-ESI-MS) as well as EA. To investigate the binding abilities of the BTCE as well as the resulting complex stability, isothermal titration calorimetry (ITC) measurements were performed. For the investigation compound **4** was utilized as model system. Since the measurement was performed in the diluted state, in a mixture of methanol and chloroform (2:1), $AgBF_4$ was selected as silver salt for this measurement based on its good solubility in organic solvents in contrast to other silver salts (e.g., $AgNO_3$). The resulting ITC-titration data are presented in the Figure S1. As assumed, the measurement revealed a stoichiometry of one BTCE to one silver ion for the formed complexes. Furthermore, within this investigation it is possible to determine the complex association (K_a) as well as dissociation constant (K_d), which were found to be $K_a = 7.03 \times 10^5$ and $K_d = 1.42 \times 10^{-6}$. The determined values proved the good applicability of the system for the desired filters. The complex association constant should be high enough to bind the silver ions from aqueous solution in a sufficient manner, but not too high so that it is still possible to recover the silver ions afterwards, which was reached by this value.

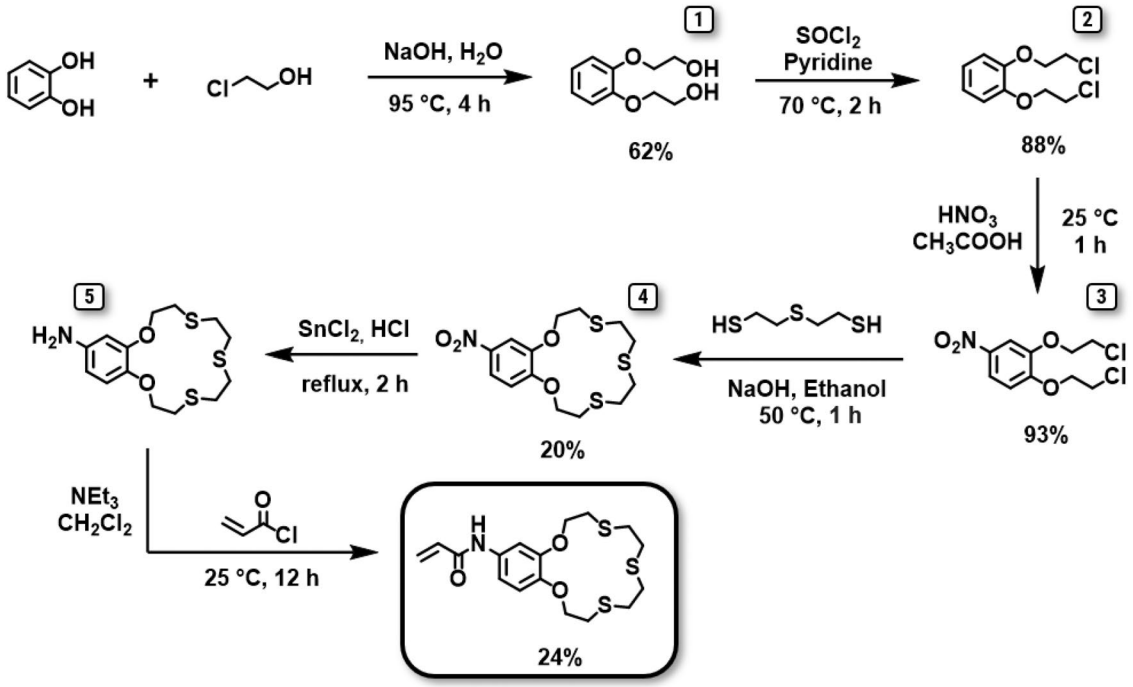

SCHEME 1 | Schematic representation of the synthesis of the benzo-15-trithiacrown-5-ether monomer (**6**).

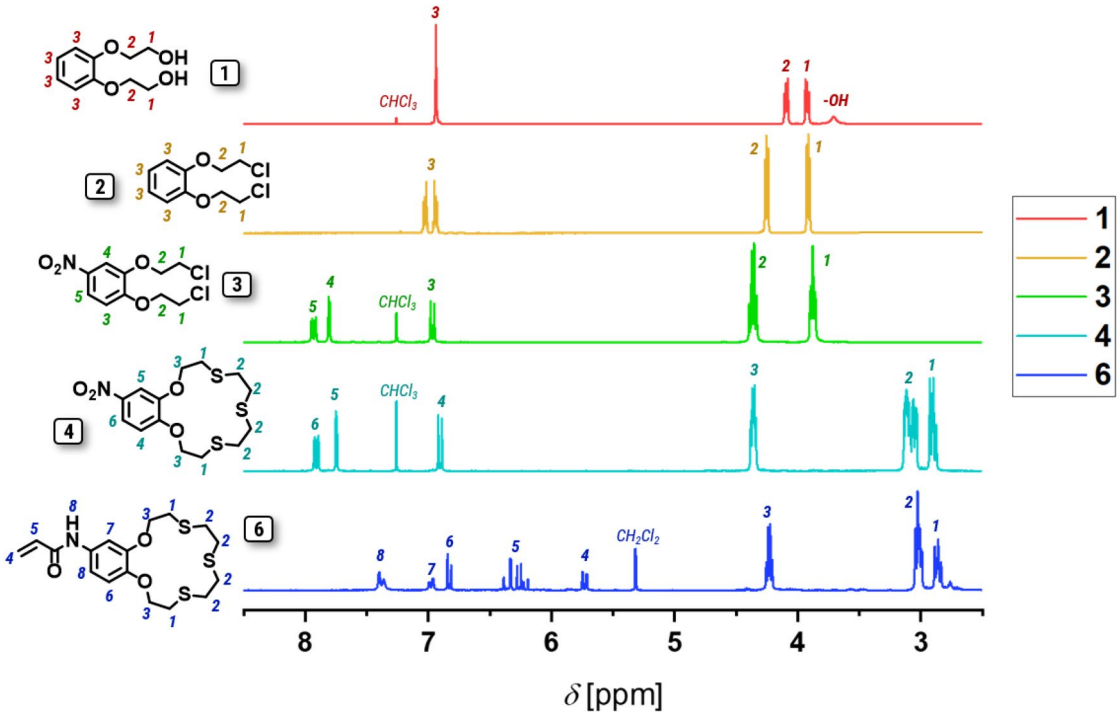

FIGURE 1 | ^{1}H NMR spectra of compounds **1** to **6**. **1**: Red, $CDCl_3$, 300 MHz. **2**: Orange, DMSO-*d6*, 400 MHz. **3**: Green, $CDCl_3$, 300 MHz. **4**: Turquoise, $CDCl_3$, 300 MHz. **6**: Blue, CD_2Cl_2, 300 MHz. [Color figure can be viewed at wileyonlinelibrary.com]

2.2 | Fabrication of the Filters

The general approach for the 3D-printing of the polymer filters is schematically presented in Figure 2. Firstly, a 3D-model was designed which is displayed in Figure 2 (top). The model was chosen based on its stable structure (hexagons) in combination with a great surface area, which is important to achieve much contact between the filter and the silver ion solution during the complexation step later on. For the 3D-printing, the synthesized BTCE monomer (**6**) as well as diphenyl(2,4,6-trimethylbenzoyl)phosphine oxide (BABO), which was utilized as photo initiator, were dissolved in the liquid monomers. As main monomer *N*,*N*-dimethyl acrylamide (DMA) was utilized, due to the high reactivity of the acrylamide functionality. Additionally, triethylene

glycol dimethacrylate (TEGDMA) was added as crosslinker to gain the required stability during the printing due to crosslinking of the forming polymer, which was selected on the basis of previous studies in which it had already shown good suitability for 3D-printing [31, 32]. The prepared monomer/initiator mixture (see Figure 2 (left)) was filled into a self-manufactured reservoir (reduced size) of the 3D-printer (Wanhao Duplicator 7 Plus, see Figure 2 (middle)) and 3D-printed within a layer-by-layer photo-polymerization approach. Different prints utilizing different amounts of the BTCE monomer (**6**) were performed. The amount of functional monomer **6** was limited by the solubility of the solid monomer in the liquid main monomers. Overall, three different filters (**F1** to **F3**) were prepared. Exemplarily, one of them is displayed in Figure 2 (right). The monomer mixtures for each filter (**F1** to **F3**) are shown in Table 1.

2.3 | Selective Complexation of Silver Ions by Filter Materials

The final goal of this study was to investigate the ability of the 3D-printed filters **F1** to **F3** to bind silver ions from aqueous solution and also to remove those ions from the polymer afterwards. Firstly, a small piece of each sample was removed and utilized for ICP-OES measurements. Afterwards, the sample was placed overnight into an aqueous solution of $AgNO_3$. Subsequently, the sample was separated from the metal ion containing solution and rinsed with deionized water. A little piece of each sample was removed and also analyzed applying ICP-OES to determine the silver-ion content bound by the filters or polymers.

For the removal of the silver ions from the polymeric materials, the samples were placed overnight into an aqueous solution of KCN and washed with deionized water afterwards. Finally, the remaining silver-ion content was also determined applying ICP-OES. A schematic representation of the complexation and decomplexation step is presented in Figure 3. The results of the ICP-OES measurements are summarized in Table 2.

The comparison of the determined silver ion content within the ICP-OES measurements before and after the treatment with $AgNO_3$ solution clearly indicates a successful complexation behavior of the presented polymeric materials.

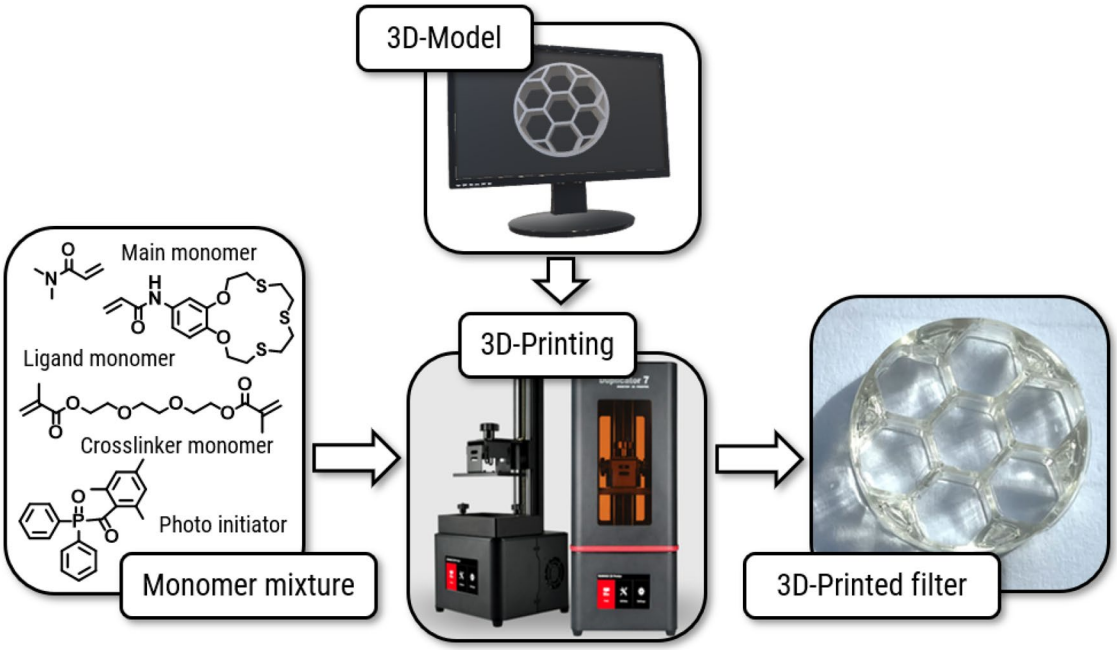

FIGURE 2 | Schematic representation of the 3D-printing of the polymer-based filters for the selective complexation of silver ions. [Color figure can be viewed at wileyonlinelibrary.com]

TABLE 1 | Utilized quantities for the 3D-printing of the filters **F1** to **F3** and the polymers resulting from the photo polymerization.

	Monomer mixture			
Sample	**DMA**	**TEGDMA**	**6**	**BAPO**
F1	1.3 g 13.11 mmol	0.56 g 1.96 mmol	20 mg 0.05 mmol	8 mg
F2			58 mg 0.15 mmol	
F3			116 mg 0.30 mmol	

Furthermore, it was found that the amount Ag^+, after the complexation step increases with the BTCE content utilized for the synthesis of them. Exemplarily, the filter **F1** (0.5% BTCE) revealed a silver-ion concentration of 2.4 mg L^{-1} after the complexation step, while for **F3** (2% BTCE) 8.8 mg L^{-1} could be achieved, which proofs the responsibility of the BTCE ligand for the fixation of the metal ions in the polymeric material. The measurements performed after the treatment with KCN solution also revealed a good removability of the silver ions from the filter.

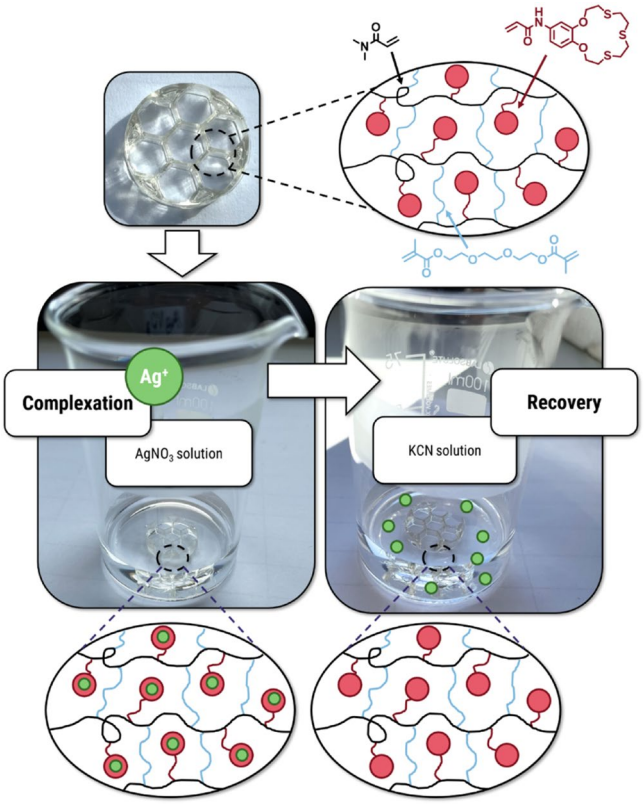

FIGURE 3 | Schematic representation of the selective complexation of silver ions in $AgNO_3$ solution (left) and the decomplexation into KCN solution (right). [Color figure can be viewed at wileyonlinelibrary.com]

It has to be noted that the theoretical values are higher compared to the determined ones after the silver complexation. This fact is not surprising, since the complexation of the metal ions is only possible at the surface of the polymeric materials. For this reason, the calculation of the theoretical values also includes the inner BTCE-moieties, which do not get in contact with the silver ions based on the overall hydrophobic character of the polymeric network. To achieve higher complexation efficiencies of the filters, it would be beneficial to extend the surface to volume ratio or to switch to a slightly more hydrophilic main monomer, which could result in a partial swelling of the filters in the aqueous solutions.

3 | Conclusion

Within this study, it was possible to develop a new approach for the fabrication of polymer filters, which are able to bind silver ions from aqueous solution. A monomer containing a benzo-15-trithia-crown-5-ether ligand was synthesized and utilized for the fabrication of polymer filters via photo 3D-printing. During the polymerizations, the content of the ligand monomer was varied resulting in three different filters. The ability of the resulting 3D-printed filters to bind silver ions was investigated in detail applying ICP-OES measurements, resulting in an increasing silver content with increasing ligand concentration in the polymer. Furthermore, also utilizing this method it was possible to show the feasibility to remove the silver-ions from the filters with KCN solution. In future, the selective complexation of other ions, such as lithium will be addressed in regard of the recycling of lithium-ion batteries.

4 | Experimental Section

4.1 | Materials and Methods

All chemicals were used as received from TCI (Eschborn, Germany), Sigma Aldrich (Darmstadt, Germany), Alfa Aesar (Kandel, Germany), Thermo Fisher Scientific (Geel, Belgium), and Acros Organics (Geel, Belgium) if not otherwise stated. All solvents were dried over molecular sieve under nitrogen

TABLE 2 | Summary of the theoretical and determined silver contents for the 3D-printed filters **F1** to **F3**.

Sample	Trithia-crown ether [%]	Step[a]	c (Ag^+) [mg L^{-1}][b]	
			Theoretical[c]	Determined[d]
F1	~0.5	Initial sample	0.0	0.130
		After Ag^+ solution	9.4	2.417
		After CN^- solution	0.0	0.104
F2	~1.0	Initial sample	0.0	0.142
		After Ag^+ solution	18.5	5.733
		After CN^- solution	0.0	0.041
F3	~2.0	Initial sample	0.0	0.347
		After Ag^+ solution	36.2	8.827
		After CN^- solution	0.0	0.099

[a]For the filters the measurements were performed with samples from the second complexation and recovery cycle.
[b]Theoretical values for a solution containing 10 mg of the filters or polymers.
[c]Maximum content calculated based on the monomer ratios utilized for the printing and photo-polymerization.
[d]Determined via ICP-OES measurements.

atmosphere. The stabilizer in the used liquid monomers (*N*,*N*-dimethyl acrylamide (DMA) and triethylene glycole dimethacrylate (TEGDMA)) was removed over a short aluminum oxide (AlOx) column (neutral AlOx, obtained from Molekula, Darlington, UK).

NMR spectra were measured using a Bruker AC 300 (300 MHz) or Bruker AC 400 (400 MHz) spectrometer (Billerica, MA, USA) at 298 K if not stated differently. The chemical shift is given in parts per million (ppm on δ scale) related to solvent residual peak.

EA was performed utilizing a Vario El III (Elementar, Langenselbold, Germany).

UV reactions were performed utilizing a UVACUBE 100 from Dr. Hoenle AG (Gilching, Germany) equipped with a mercury lamp.

Microwave-assisted reactions were performed in capped microwave vials (2 to 5 mL) using a Biotage Initiator-8 microwave synthesizer (max. power of 400 W, working frequency of 4.45 GHz).

All titrations were performed using a standard volume Nano ITC (TA Instruments) at 303 K. Solutions were always prepared prior to use in dry solvent using vacuum dried ligand and metal salt. Blank titrations in dry solvent were performed and subtracted from the corresponding titrations to remove the effect of dilution. The fitting of the measured data were performed with the NanoAnalyze program from TA instruments.

Inductively coupled plasma optical emission spectroscopy (ICP-OES) measurements were performed using an ICP-OES spectrometer 725ES (Agilent, Waldbronn, Germany) with a CCD-detector equipped with an auto-sampler ASX 520 (Teledyne CETAC, Omaha, USA), a seaspray nebulizer, twister cyclonic spray chamber, argon humidifier and 1.4 mm id injector tube for radial ICP. The applied gas stream was 0.74 L/min for the nebulizer, 16.5 L min^{-1} for the plasma gas and 1.5 L min^{-1} for supporting gas. The calibration was performed using ICP multi-element standard solution IV from VWR (1.11355.0100). The applied wavelengths were 328.068 nm. The correctness was checked using a multi-element standard from Bernd Kraft (17 elements in nitric acid). Each measurement was repeated three times with 10 s integration time. The average value was utilized.

4.2 | Synthesis of Benzo-15-Trithiacrown-5-Ether Monomer

The synthesis of the benzo-15-trithiacrown-5-ether monomer was adapted from reported literature procedures [27].

4.2.1 | Synthesis of 1,2-*Bis*(2-Hydroxyethoxy) Benzene (1)

The reaction was performed under nitrogen atmosphere. 2-Chloroethanol (17.6 g, 217.96 mmol) and catechol (4.0 g, 36.33 mmol) were diluted in water (40 mL) and a solution of NaOH (8.7 g, 217.98 mmol) in water (120 mL) was added. Subsequently, the solution was stirred for 4 h at 95°C and, afterwards, cooled to room temperature. Concentrated H_2SO_4 (1 mL) was added before the reaction mixture was extracted three times with chloroform (100 mL). The organic layer was dried over Na_2SO_4 and the crude product was further purified via gel chromatography (silica, ethyl acetate) to yield **1** (4.5 g, 62%) as a white solid.

^{1}H NMR (300 MHz, $CDCl_3$, δ): 3.71 (s, 1H, -O*H*), 3.92 (dd, J = 5.0; 3.6 Hz 4H, -CH_2-OH), 4.09 (dd, J = 4.9; 3.7 Hz, 4H, -O-CH_2), 6.94 (s, 4H, Ar-*H*) ppm.

^{13}C NMR (75 MHz, $CDCl_3$, δ): 61.1 (-*C*H_2-OH), 71.5 (-O-*C*H_2), 114.9 (Ar-*C*), 122.1 (Ar-*C*), 148.9 (Ar-*C*-O) ppm.

Anal. calcd. for $C_{10}H_{14}O_4$: C 60.59, H 7.12; found: C 60.62, H 7.26.

4.2.2 | Synthesis of 1,2-*Bis*(2-Chloroethoxy) Benzene (2)

Compound **1** (2.0 g, 10.99 mmol) was placed in a flask and pyridine (1.33 mL, 16.48 mmol) was added. Thionyl chloride (2.5 g, 21.37 mmol) was added dropwise before the mixture was stirred for 2 h at 70°C. Afterwards, the reaction mixture was extracted three times with toluene (100 mL). Thereafter, the organic layer was washed three times with water and dried over Na_2SO_4. The solvent was removed under reduced pressure to yield **2** (2.1 g, 88%) as white solid, which was utilized without further purification.

^{1}H NMR (400 MHz, DMSO-*d6*, δ): 3.91 (m, 4H, -CH_2-Cl), 4.25 (m, 4H, -O-CH_2), 7.10–6.88 (m, 4H, Ar-*H*) ppm.

^{13}C NMR (75 MHz, DMSO-*d6*, δ): 43.2 (-*C*H_2-Cl), 69.4 (-O-*C*H_2-), 115.7 (Ar-*C*), 122.1 (Ar-*C*), 148.1 (Ar-*C*-O-) ppm.

Anal. calcd. for $C_{10}H_{12}O_2Cl_2$: C 51.09, H 5.14, Cl 30.16; found: C 50.07, H 5.10, Cl 29.03.

4.2.3 | Synthesis of 1,2-*Bis*(2-Chloroethoxy)-4-Nitrobenzene (3)

Compound **2** (6.0 g, 25.52 mmol) was mixed under stirring with concentrated acetic acid (3.7 mL). Subsequently, HNO_3 (9.7 mL, 65%) was added dropwise. Afterwards, the reaction mixture was stirred for 1 h at room temperature. The product was precipitated from water (800 mL), filtered, washed two times with water and dried in vacuo at a temperature of 40°C. **3** (6.6 g, 93%) was obtained as yellow solid.

^{1}H NMR (300 MHz, $CDCl_3$, δ): 3.88 (td, J = 5.8; 1.7 Hz, 4H, -CH_2-Cl), 4.36 (dd, J = 12.5; 5.9 Hz, 4H, -O-CH_2), 6.97 (d, J = 8.9 Hz, 1H, Ar-*H*), 7.81 (d, J = 2.6 Hz, 1H, Ar-*H*), 7.93 (dd, J = 8.9; 2.6 Hz, 1H, Ar-*H*) ppm.

^{13}C NMR (75 MHz, $CDCl_3$, δ): 41.6 (*C*H_2-Cl), 41.8 (*C*H_2-Cl), 69.6 (-O-*C*H_2), 70.0 (-O-*C*H_2), 110.4 (Ar-*C*), 113.2 (Ar-*C*), 118.8 (Ar-*C*), 142.1 (Ar-*C*-NO_2), 148.1 (Ar-*C*-O), 154.0 (Ar-*C*-O) ppm.

Anal. calcd. for $C_{10}H_{12}NO_4Cl_2$: C 42.88, H 3.96, N 5.00, Cl 25.31; found: C 43.04, H 3.93, N 4.87, Cl 24.91.

4.2.4 | Synthesis of 2,3-(4′-Nitrobenzo)-7,10,13-Trithia-1,4-Dioxa-Cyclopentadeca-2-En (4)

The reaction was performed under nitrogen atmosphere. A solution of NaOH (1.0 g, 25.00 mmol) and 2.2′-thioethane thiol (1.1 g, 7.13 mmol) in dry ethanol (100 mL) was heated to 50°C. Subsequently, a solution of Compound **3** (2.0 g, 7.14 mmol) in warm ethanol (200 mL) was added dropwise. The reaction mixture was stirred for 1 h at 50°C and afterwards filtered hot. The organic layer was placed in the fridge overnight. The resulting precipitation was filtered and recrystallized in *n*-heptane, leading to the product **4** (0.51 g, 20%) as yellow solid.

^{1}H NMR (300 MHz, $CDCl_3$, δ): 3.18–2.79 (m, 12H, -CH_2-), 4.36 (dd, J = 9.1; 3.7 Hz, 4H, -O-CH_2-), 6.90 (d, J = 9.0 Hz, 1H, Ar-*H*), 7.75 (d, J = 2.6 Hz, 1H, Ar-*H*), 7.91 (dd, J = 8.9; 2.6 Hz, 1H, Ar-*H*) ppm.

^{13}C NMR (75 MHz, $CDCl_3$, δ): 31.5 (-CH_2-), 33.4 (-CH_2-), 33.5 (-CH_2-), 33.6 (-CH_2-), 72.4 (-O-CH_2-), 72.6 (-O-CH_2-), 107.6 (Ar-*C*), 111.0 (Ar-*C*), 118.1 (Ar-*C*), 141.7 (Ar-*C*-NO_2), 148.2 (Ar-*C*-O-), 153.9 (Ar-*C*-O-) ppm.

Anal. calcd. for $C_{14}H_{19}NO_4S_3$: C 46.52, H 5.30, N 3.87, S 26.61; found: C 46.29, H 5.23, N 3.91, S 24.83.

4.2.5 | Synthesis of 2,3-(4′-Aminobenzo)-7,10,13-Trithia-1,4-Dioxa-Cyclopentadeca-2-En (5)

Compound **4** (1.0 g, 2.78 mmol) was dissolved in ethanol (200 mL) under reflux. Subsequently, hydrochloric acid (56 mL, 37%) and tin(II) chloride (1.7 g, 8.70 mmol) were added. The reaction mixture was stirred for 2 h under reflux. Afterwards, the mixture was poured into ice water and neutralized with NH_3. The resulting aqueous phase was extracted three times with dichloromethane (100 mL). The organic layer was dried over Na_2SO_4 and the solvent was removed under reduced pressure. The resulting crude product (**5**) was used without further purification.

4.2.6 | Synthesis of 2,3-(4′-Acrylamidobenzo)-7,10,13-Trithia-1,4-Dioxa-Cyclopentadeca-2-En (6)

The reaction was performed under nitrogen atmosphere. Acryloyl chloride (0.6 g, 6.31 mmol) was added dropwise to a solution of the crude product **5** and triethylamine (0.4 mL, 3.01 mmol) in dichloromethane (100 mL). The reaction mixture was stirred for 12 h at room temperature, followed by washing steps with saturated aqueous $NaHCO_3$ (two times) and NaCl (three times) solution. The organic layer was dried over Na_2SO_4 and the solvent was removed under reduced pressure. The final product **6** (0.5 g, 24%) was obtained as white solid after gel chromatography (silica, *n*-hexane/ethyl acetate (1:1)).

^{1}H NMR (300 MHz, CD_2Cl_2, δ): 2.96–2.77 (m, 4H, -O-CH_2–CH_2-S), 3.13–2.92 (m, 8H, -S-CH_2-), 4.23 (dd, J = 9.9, 4.8 Hz, 1H, -O-CH_2-), 5.73 (dd, J = 9.8, 1.8 Hz, 1H, Allyl-*H*), 6.83 (d, J = 8.7 Hz, 1H, Ar-*H*), 6.47–6.03 (m, 1H, Allyl-*H*), 7.49–7.25 (m, 2H, Ar-*H*, N*H*), 6.98 (dd, J = 8.6; 2.2 Hz, 1H, Ar-*H*) ppm.

HRMS (ESI) m/z: $[M+Na]^+$ calcd. for $C_{17}H_{23}NO_3S_3$, 408.07; found, 408.08.

Anal. calcd. for $C_{17}H_{23}NO_3S_3$: C 52.69, H 6.01, N 3.58, S 24.95; found: C 53.34, H 6.14, N 3.58, S 24.16.

4.3 | 3D-Printing and Photo Polymerization

In order to reduce the required monomer amount for the printing process, a self-manufactured reservoir as well as plate was utilized for the 3D-printing of the polymer filters **F1** to **F3**. Photos of the modified 3D-printer are shown in the Supporting Information.

The synthesized monomer **6**, as well as the photo-initiator diphenyl(2,4,6-trimethyl benzoyl) phosphine oxide (BABO) were dissolved in a mixture of the liquid monomers DMA and TEGDMA. A molar monomer to initiator ratio of 1000 to 1 was utilized for all 3D-prints regarding all photocurable monomers in the reaction mixture. Subsequently, the mixture was filled into the self-manufactured reservoir and the 3D-printing was started. All utilized quantities of the printing processes are listed in Table 1.

The 3D-printing was performed using a Wanhao Duplicator 7 Plus (wavelength: 405 nm, layer thickness: 30 µm, cure time: 50 s). A table summarizing all printing parameters can be found in the Supporting Information. The 3D-model was sliced by Wanhao D7 WorkShop Version 2.1.3. The 3D-printed model was carefully removed from the printing plate and washed with acetone.

4.4 | Complexation and Decomplexation of Silver Ions

Complexation: For the complexation of silver ions, the printed polymer was placed over night in aqueous $AgNO_3$-solution (150 mL, 0.01 mol L^{-1}) and rinsed with deionized water afterwards.

Decomplexation: For decomplexation the prior complexed polymer was placed overnight in aqueous KCN-solution (150 mL, 0.01 mol L^{-1}) and rinsed with deionized water.

Preparation of ICP-OES solutions: The respective polymer (approx. 20 mg) was added to a solution of 800 µL nitric acid (65%) and 200 µL hydrogen peroxide (30%) and heated for 15 min at 180°C utilizing a microwave (10 s prestirring, 12 bar, 300 W). Afterwards, the solution was transferred and diluted in a 10 mL volumetric flask using 1% nitric acid and characterized via inductively coupled plasma optical emission spectroscopy (ICP-OES) Table 3.

TABLE 3 | Results of the ICP-OES measurements for the 3D-printed filters **F1** to **F3**.

Sample	Trithia-crown ether [%]	Step[a]	Sample mass [mg]	ICP-OES results	
				Ag^+ [mg L^{-1}]	SD[b] [mg L^{-1}]
F1	~0.5	Initial sample	12.8	0.166	0.002
		After Ag^+ solution	12.0	2.900	0.0001
		After CN^- solution	10.3	0.107	0.0003
F2	~1.0	Initial sample	11.7	0.166	0.001
		After Ag^+ solution	12.0	6.880	0.02
		After CN^- solution	19.2	0.078	0.001
F3	~2.0	Initial sample	13.0	0.451	0.003
		After Ag^+ solution	13.2	11.651	0.003
		After CN^- solution	12.6	0.125	0.002

[a]For the filters the measurements were performed with samples from the second complexation and recovery cycle.
[b]Standard deviation.

Author Contributions

Timo Koswig: data curation (lead), formal analysis (lead), writing – original draft (lead). **Josefine Meurer:** data curation (equal), writing – original draft (equal). **Thomas Bätz:** data curation (equal), writing – original draft (equal). **Oswald Müschke:** data curation (supporting). **Stefan Zechel:** supervision (equal), writing – review and editing (equal). **Martin D. Hager:** supervision (equal), writing – review and editing (equal). **Ulrich S. Schubert:** conceptualization (equal), funding acquisition (lead), supervision (lead), writing – original draft (lead).

Acknowledgments

J.M. and T.S. contributed equally to this work. The authors would like to thank the Carl Zeiss Stiftung (Durchbrüche 2019). Open Access funding enabled and organized by Projekt DEAL.

Conflicts of Interest

The authors declare no conflicts of interest.

Data Availability Statement

The data that support the findings of this study are available from the corresponding author upon reasonable request.

References

1. I. Leksic, N. Stefanic, and I. Veza, "The Impact of Using Different Lean Manufacturing Tools on Waste Reduction," *Advances in Production Management* 15 (2020): 81.

2. A. Dorigato, "Recycling of Polymer Blends," *Advanced Industrial and Engineering Polymer Research* 4 (2021): 53–69.

3. L. Shen and E. Worrell, "Chapter 31—Plastic Recycling," in *Handbook of Recycling*, Second ed., eds. C. Meskers, E. Worrell, and M. A. Reuter (Amsterdam, Netherlands: Elsevier, 2024), 497.

4. I. A. Ignatyev, W. Thielemans, and B. V. Beke, "Recycling of Polymers: A Review," *ChemSusChem* 7 (2014): 1579–1593.

5. A. K. Mohanty, F. Wu, R. Mincheva, et al., "Sustainable Polymers," *Nature Reviews Methods Primers* 2 (2022): 46.

6. Y. Miao, L. Liu, Y. Zhang, Q. Tan, and J. Li, "An Overview of Global Power Lithium-Ion Batteries and Associated Critical Metal Recycling," *Journal of Hazardous Materials* 425 (2022): 127900.

7. L. Carlsen, "Sustainability: An Ethical Challenge: The Overexploitation of the Planet as an Exemplary Case," *Sustainability* 16 (2024): 3390.

8. B. K. Reck and T. E. Graedel, "Challenges in Metal Recycling," *Science* 337 (2012): 690–695.

9. E. Lahtinen, L. Kivijärvi, R. Tatikonda, A. Väisänen, K. Rissanen, and M. Haukka, "Selective Recovery of Gold From Electronic Waste Using 3D-Printed Scavenger," *American Chemical Society Omega* 2 (2017): 7299–7304.

10. K. Ibebunjo, Y. El Ouardi, J. Kwame Bediako, A. Iurchenkova, and E. Repo, "Functionalization of Recycled Polymer and 3D Printing Into Porous Structures for Selective Recovery of Copper From Copper Tailings," *Chemical Engineering Science* 286 (2024): 119664.

11. E. Lahtinen, M. M. Hänninen, K. Kinnunen, et al., "Porous 3D Printed Scavenger Filters for Selective Recovery of Precious Metals From Electronic Waste," *Advanced Sustainable Systems* 2 (2018): 1800048.

12. N. Shahrubudin, T. C. Lee, and R. Ramlan, "An Overview on 3D Printing Technology: Technological, Materials, and Applications," *Procedia Manufacturing* 35 (2019): 1286–1296.

13. M. Zastrow, "3D Printing Gets Bigger, Faster and Stronger," *Nature* 578 (2020): 20–23.

14. D. T. Pham and C. Ji, "Design for Stereolithography," *Proceedings of the Institution of Mechanical Engineers, Part C* 214 (2000): 635.

15. M. Oleksy, K. Dynarowicz, and D. Aebisher, "Rapid Prototyping Technologies: 3D Printing Applied in Medicine," *Pharmaceutics* 15 (2023): 2169.

16. J. Z. Manapat, Q. Chen, P. Ye, and R. C. Advincula, "3D Printing of Polymer Nanocomposites via Stereolithography," *Macromolecular Materials and Engineering* 302 (2017): 1600553.

17. B. Berman, "3-D Printing: The New Industrial Revolution," *Business Horizons* 55 (2012): 155–162.

18. S. Lawson, X. Li, H. Thakkar, A. A. Rownaghi, and F. Rezaei, "Recent Advances in 3D Printing of Structured Materials for Adsorption and Catalysis Applications," *Chemical Reviews* 121 (2021): 6246–6291.

19. Z. Zhao, X. Tian, and X. Song, "Engineering Materials With Light: Recent Progress in Digital Light Processing Based 3D Printing," *Journal of Materials Chemistry C* 8 (2020): 13896–13917.

20. S. H. Masood, "Intelligent Rapid Prototyping With Fused Deposition Modelling," *Rapid Prototyping Journal* 2 (1996): 24–33.

21. O. A. Mohamed, S. H. Masood, and J. L. Bhowmik, "Optimization of Fused Deposition Modeling Process Parameters: A Review of Current Research and Future Prospects," *Advanced Manufacturing* 3 (2015): 42–53.

22. D. A. Komissarenko, P. S. Sokolov, A. D. Evstigneeva, et al., "DLP 3D Printing of Scandia-Stabilized Zirconia Ceramics," *Journal of the European Ceramic Society* 41 (2021): 684–690.

23. Y. Gok, "The Synthesis and Characterization of New Substituted Diaminoglyoxime and Its Cobalt(III) Complexes Containing 15-Membered Dioxa-Trithia Macrocyclic Moieties," *Polyhedron* 15 (1996): 3933–3940.

24. M. Oue, K. Kimura, and T. Shono, "Extraction-Spectrofluorimetric Determination of Silver Ion Using Benzothiacrown Ether and Eosin," *Analyst* 113 (1988): 551.

25. M. Oue, K. Kimura, and T. Shono, "Liquid-Liquid Extraction of Silver Ion With Benzothiacrown Ether Derivatives," *Analytica Chimica Acta* 194 (1987): 293–298.

26. S. Singha, D. Kim, H. Seo, S. W. Cho, and K. H. Ahn, "Fluorescence Sensing Systems for Gold and Silver Species," *Chemical Society Reviews* 44 (2015): 4367–4399.

27. M. Oue, A. Ishigaki, K. Kimura, Y. Matsui, and T. Shono, "Synthesis and Cation-Binding Properties of Poly-and Bis(thiacrown ether)s," *Journal of Polymer Science, Polymer Chemistry Edition* 23 (1985): 2033–2042.

28. Y. He, F. Wang, X. Wang, J. Zhang, D. Wang, and X. Huang, "A Photocurable Hybrid Chitosan/Acrylamide Bioink for DLP Based 3D Bioprinting," *Materials and Design* 202 (2021): 109588.

29. I. Isarn, Ľ. Hodásová, M. M. Pérez-Madrigal, F. Estrany, E. Armelin, and F. Bravo, "Digital Light Processing-3D Printing of Thermoset Materials With High Biodegradability From Amino Acid-Derived Acrylamide Monomers," *Macromolecular Rapid Communications* 44 (2023): 2300132.

30. Y. Wang, Z. Wang, S. Liu, et al., "Additive Manufacturing of Silica Ceramics From Aqueous Acrylamide Based Suspension," *Ceramics International* 45 (2019): 21328–21332.

31. J. Meurer, R. H. Kampes, T. Bätz, et al., "3D-Printable Shape-Memory Polymers Based on Halogen Bond Interactions," *Advanced Functional Materials* 32 (2022): 2207313.

32. C.-H. Lin, Y.-M. Lin, Y.-L. Lai, and S.-Y. Lee, "Mechanical Properties, Accuracy, and Cytotoxicity of UV-Polymerized 3D Printing Resins Composed of Bis-EMA, UDMA, and TEGDMA," *Journal of Prosthetic Dentistry* 123 (2020): 349–354.

Supporting Information

Additional supporting information can be found online in the Supporting Information section.